11 Intensity Statistics of the Light Scattered by Particles on Surfaces

E.M. Ortiz, F. González, and F. Moreno

Departamento de Física Aplicada. Grupo de Óptica.
Universidad de Cantabria. 39005 Santander (SPAIN)

Abstract. Researchers have studied the statistics of the fluctuations of the scattered intensity from a small number of non-interacting particles for many years. For such samples, the statistics deviate from typical Gaussian behaviour and the normalized moments of the fluctuations of the scattered intensity become a function of the mean number of scatterers in the illuminated area. For instance, the measurement of the second moment provides a simple method for determining the scatterer surface density. In this chapter, we present an extension of these studies by including the interaction between the scatterers. In particular, we focus on systems consisting of isotropic and non-isotropic particles located on flat substrates. We demonstrate that the probability of detecting zeros in the cross-polarized scattered intensity can be a useful characterizing tool.

1 Introduction

The statistics of the intensity of light scattered by surface and volume diffusers have been studied for many years. Laser speckle is a very well known phenomenon. A theoretical and experimental background of this phenomenon can be found in [1]. In most of the contributions contained in this book and in other works, it is assumed that the number of scattering centers contributing to the total scattered field is so large that, under the scalar approximation, the central limit theorem is applicable. In these cases, multiple scattering effects are not included, and the total amplitude of the scattered electric field can be calculated by means of a random-walk procedure. The statistics follow a Rayleigh distribution typical of a random, complex, circular, Gaussian process. The corresponding scattered-intensity statistics can also be calculated in a straightforward manner and the result shows that the probability density function (PDF) is an exponential whose normalized moments are given by the simple factorial law

$$\frac{\langle I^n \rangle}{\langle I \rangle^n} = n! \tag{1}$$

For such Gaussian processes, the normalized second moment takes on the value of 2. This means that the signal-to-noise ratio, or the contrast of the signal, is unity. For such a low signal-to-noise ratio, it is very difficult to get any information about the diffuser from the statistical analysis of

F. Moreno and F. González (Eds.): Lectures 1998, LNP 534, pp. 191–211, 2000.

the scattered intensity. However, when the size of the illuminated area (or volume) is small and only a few scatterers contribute to the total scattered field, the statistics no longer remain Gaussian. It then becomes possible to extract more information from the scatterer. An excellent review of non-Gaussian scattering processes with no scatterer interaction is contained in [2].

Non-Gaussian processes are especially interesting when the diffuser is composed of discrete scattering centers. This is because it is possible to obtain direct information of the density of scattering centers from an experimental analysis of the statistics of the scattered intensity, and in particular the normalized second moment, $< I^2 > / < I >^2$ [2]. Until recently, most of the studied systems do not take multiple interaction into account.

The purpose of this chapter is to introduce the reader to the theoretical background of non-Gaussian processes when the diffusing targets contain discrete scattering centers and multiple interaction is included. The questions are how the scatterer interaction changes the statistics of the scattered light intensity and what information can be obtained from the analysis of the resulting statistics. In particular, we introduce a statistical method based on the measurement of the probability of detecting a null intensity in the cross-polarized scattered light. We focus our study on surfaces seeded with small particles because of their practical applications (surface contamination [3], the semiconductor industry [4], Surface Enhanced Raman Spectroscopy [5], etc.) and because this can be considered a simple model for more complex random natural surfaces [6]. Both isotropic and anisotropic scatterers are analyzed.

This chapter is organized as follows. In Sect. 2, we present the scattering model we use along with the mathematical tools and models that are used in the numerical calculations. Section 3 provides a theoretical basis to understand the intensity fluctuations of the resulting scattered light calculated without considering multiscattering effects. Section 4 introduces a simple model that accounts for the interaction between particles when they are on a substrate. Finally, in Sect. 5 we present an empirical study of the statistics of the scattered intensity when scatterer interaction is important. In this case, scatterer anisotropy is also considered.

2 The Scattering Model

2.1 Scattering Geometry

The scattering model is shown in Fig. 1. It consists of a flat surface that separates two semi-infinite media of dielectric constants $\varepsilon_1$and ε_2. This surface is contaminated with particles, either isotropic or anisotropic, whose size is much smaller than the incident wavelength λ. If the particles are isotropic in nature (spheres), they are characterized by a radius a and dielectric constant ε_p in such a way that their polarizability α is given by [7]

$$\alpha = 4\pi a^3 \frac{\varepsilon_p - \varepsilon_1}{\varepsilon_p + 2\varepsilon_1} \tag{2}$$

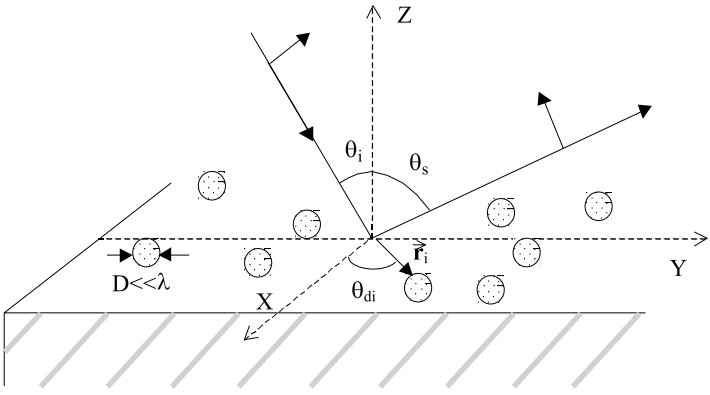

Fig. 1. Scattering geometry.

Anisotropic particles are characterized by a polarizability tensor $\|\alpha\|$, which is diagonal in the coordinate system given by the directions of the three main axes of the particle. The three diagonal elements of this tensor, α_x, α_y and α_z, are given by [7]

$$\alpha_i = V \frac{\varepsilon_p - \varepsilon_1}{\varepsilon_1 + L_i\left(\varepsilon_p - \varepsilon_1\right)},\ i = x, y, z \tag{3}$$

where V is the particle volume and $L_i (i = x, y, z)$ are geometrical factors satisfying the relation $L_x + L_y + L_z = 1$ [8].

The system is illuminated by a plane wave at an incidence angle θ_i measured from the surface normal. The plane of incidence coincides with the YZ plane and the scattered intensity is analyzed in this plane at scattering angle θ_s as shown in Fig. 1. We consider two linear polarization states of the incident wave, either perpendicular (S polarization) or parallel (P polarization) to the plane of incidence. Similarly, we consider the same two linear polarization (analyzer) states for the scattered wave in the plane of incidence. The co-polarized case when both incident and scattered electric fields are parallel is referred to as either SS or PP. Similarly, the cross-polarized case when they are perpendicular is referred to as either SP or PS.

2.2 The Perfect Conductor Approximation and the Image Theory

One of the most common approximations used to solve electromagnetic scattering problems near rough surfaces is to assume that the surface behaves as a perfect conductor ($\varepsilon_2 = -\infty$). There are several reasons for using this approximation. The most important is that the computation is greatly simplified. Obviously, the adoption of this approximation must have some physical meaning, and the results do have greater validity for metallic surfaces than for dielectric ones. However, depending on the problem, the optical properties of the surface are often irrelevant and we are justified in using the perfect-conductor approximation (PCA). For example, the most relevant physical aspects of the well-known enhanced-backscattering effect can be explained by assuming that the rough surface is perfectly conducting [9]. Similarly, the study of the statistics of the scattered intensity by particles on substrates does not depend significantly on the substrate refractive index. In this case, the use of the PCA has several advantages. For instance, with this approximation and for the scattering geometry shown in Fig. 1, the image method (IM) introduced by Rayleigh [10] provides exact results for the scattered field. According to this method, the scattering problem of one small particle located on a flat, perfectly conducting substrate illuminated by a plane wave is completely equivalent to having two particles (one the image of the other with respect to the substrate surface) illuminated by two plane waves (the originally incident wave and its image with respect to the surface plane) whose phase relationship is given by the boundary conditions at the perfectly conducting interface. Figure 2 gives a clear idea of how the image method works. The PCA and the IM constitute the basis of the calculations presented throughout this chapter.

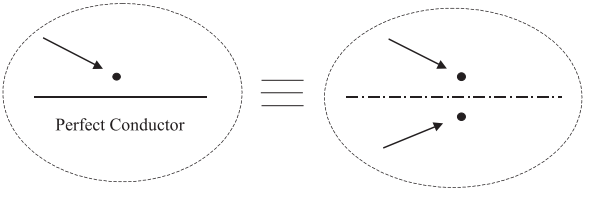

Fig. 2. Two equivalent scattering problems according to the Image Method (IM) introduced by Lord Rayleigh [10].

3 Intensity Fluctuations. Non-interacting Particles

Scattering systems formed by particles or discrete scatterers constitute a basic model for studying scattered intensity fluctuations. For the case of small, non-interacting particles, under the scalar approximation (only S or P polarized light is detected) the scattered electric (magnetic) field amplitude in the far-field region in a certain scattering direction is given by

$$A = \sum_{i=1}^{N} a_i \exp(i\varphi_i) \tag{4}$$

where N is the number of particles contributing to the scattered field, a_i is the electric (magnetic) field amplitude of the scattered wave by particle i and φ_i is its phase measured with respect to an arbitrary origin. From Fig. 1, if r_i and θ_{d_i} denote the position of particle i (in polar coordinates) with respect to this origin, φ_i can be written as

$$\varphi_i = k r_i \sin\theta_s \sin\theta_{d_i} \tag{5}$$

where $k = 2\pi/\lambda$ and the rest of the parameters can be found explicitly in Fig. 1. We assume that the amplitudes a_i and phases φ_i of (4) are independent and that the cross-correlation terms $\langle \varphi_i \varphi_j \rangle$ and $\langle a_i a_j \rangle$ are equal to zero when $i \neq j$. This is a consequence of the assumption that the particles are non-interacting. Furthermore, the random distribution of the positions of the particles, given by r_i and θ_{d_i}, are assumed to give the corresponding phases φ_i uniformly distributed over 2π radians. If N is fixed in the illuminated area, fluctuations in the scattered intensity are due to the randomness of a_i and φ_i when we consider different samples by illuminating different parts of the scattering surface. It has been shown [11] that the probability of detecting a scattered intensity between I and $I + dI$ ($I \propto |A|^2$) can be expressed as

$$P(I)dI = \frac{1}{2} \int_0^\infty \xi J_0(\xi\sqrt{I}) \left\langle J_0(\xi a) \right\rangle^N d\xi dI \tag{6}$$

where J_0 is the Bessel function of zero order. For brevity, we do not show the details of the derivation of (6), which can be found in [11]. This equation is obtained under the assumption that the individual scattering amplitudes, a_i, of (4) are fluctuating ($\langle\rangle$ in (6) means an ensemble average over the different distributions of a_i), statistically independent and statistically identical. The calculation of the moments of the distribution function of (6) is straightforward and gives the following results for the first two moments

$$\langle I \rangle = N \left\langle a^2 \right\rangle \tag{7}$$

$$\frac{\langle I^2 \rangle}{\langle I \rangle^2} = 2\left(1 - \frac{1}{N}\right) + \frac{1}{N}\frac{\langle a^4 \rangle}{\langle a^2 \rangle^2}. \tag{8}$$

Apart from the obvious result given by (7), (8) for the second moment indicates that when N is fixed and remains small enough, fluctuations in the scattered intensity can be enhanced due to fluctuations in the scattering amplitudes a_i. Enhancement is only possible if the scattering centers are anisotropic in nature and randomly oriented (since we are considering small particles). This enhancement depends not only on the number of scattering centers (i.e., the size of the illuminated area) but also on the statistics of a_i. However, for spherical symmetry $\langle a^4 \rangle = \langle a^2 \rangle^2$, so

$$\langle I^2 \rangle / \langle I \rangle^2 = 2 - \frac{1}{N} \tag{9}$$

and instead of observing enhanced fluctuations, we get reduced fluctuations (i.e., $\langle I^2 \rangle / \langle I \rangle^2 < 2$) and the speckle contrast is considerably reduced as $N \to 1$**.** This means that as $N \to 1$, it becomes harder to see a clear distinction between maxima and minima in the speckle field. In any case, when N tends to infinity, the probability density function $P(I)$ tends to an exponential, and its second factorial moment tends to the value of 2, typical of a Gaussian statistical process. In this case all the information concerning both the number of scattering particles (both terms of (8)) and their scattering properties (second term of (8)) is completely lost. On the other hand, in the non-Gaussian regime, i.e. when N is small in the illuminated area, the measurement of $\langle I^2 \rangle / \langle I \rangle^2$ can provide information not only about the particle surface density but also about how these particles scatter the incident light beam, and therefore, about the particles themselves.

An interesting problem arises when the number of particles in the illuminated area is not fixed but fluctuates. For instance, if the geometry shown in Fig. 1 is illuminated by a small spot of light (in principle, we assume an illuminating beam with a hard-edge profile which, for our calculation purposes, can model a real Gaussian beam profile) and we get scattering intensity samples by scanning the illuminating spot over the surface, the number of illuminated particles will fluctuate from region to region. If the particle surface density ρ is uniform, the fluctuations of the particle number N can be modeled very well by a Poisson statistical process with mean

$$\bar{N} = \pi \rho R^2 / \cos\theta_i, \tag{10}$$

R being the illuminating spot radius. The new expression for $P(I)$ can be found by averaging (6) over a Poisson process with the mean given by (10) [11] (only isotropic particles are considered)

$$P(I)dI = \frac{1}{2}\int_0 \zeta J_o(\zeta\sqrt{I}) \exp\left\{\bar{N}\left[J_o(\zeta a) - 1\right]\right\} d\zeta dI \tag{11}$$

whose second factorial moment (the first moment is not interesting since it is simply proportional to $\bar{N}$) is given by

$$\left\langle I^2\right\rangle / \left\langle I\right\rangle^2 = 2 + 1/\bar{N} \tag{12}$$

For isotropic scatterers, it is interesting to compare (9) and (12) and to observe that particle number fluctuations enhance those of the scattered intensity in such a way that in contrast to what happens for fixed N, the speckle contrast increases as $\overline{N}$ decreases.

4 Particle Interaction. A Simple Model

The main objective of this chapter is to show how the statistics of the scattered intensity from surfaces like that of Fig. 1 change when the interaction between the scatterers is included. In this section, we introduce a simple model for analyzing the multiple scattering effects on the scattered intensity in the plane of incidence: changes in the co-polarized light, appearance of cross-polarized light, etc. A knowledge of the interaction between the scatterers, its range, its strength, etc., is the first step towards understanding the final and most important part of this chapter.

The basis of the model consists of three elements: the perfect-conductor approximation (PCA), the image method (IM) (see Sect. 2.2) and the coupled-dipole method (CDM), also known in the literature as the discrete-dipole approximation (DDA) (see the Introduction chapter). As previously outlined, the adoption of the PCA for the substrate allows us to use the IM as an exact method for calculating the scattered far field. As a result, the geometry of Fig. 1 can be replaced by one of two parallel planes of particles separated by twice the radius of the particles (for isotropic scatterers) and illuminated by two plane waves, one the image of the other taking into account the boundary conditions at the perfect conductor interface. The CDM is now introduced not only to consider the interaction between a particle and its neighbors, but also the interaction of a particle with itself due to the presence of the substrate.

The CDM has been widely and successfully used to calculate the scattered field from particles with irregular shapes, for which an analytical approach to the electromagnetic problem is impossible. For the cases we are analyzing, this method is especially advantageous because, for the geometry of Fig. 1, the problem of calculating the local field in every particle (dipole) is simplified, i.e. $2N$ dipole units (N is the number of illuminated particles) distributed

randomly in two parallel planes, one the image of the other, separated by a distance $2a$, a being the particle radius. The local electric field in particle i is given by

$$\overrightarrow{E_i} = \overrightarrow{E_i^o} + \sum_{j \neq i}^{2N} \left\{ A_{ij} \left\| \alpha \right\|_j \overrightarrow{E_j} + B_{ij} \left[\left(\left\| \alpha \right\|_j \overrightarrow{E_j} \right) \overrightarrow{n_{ji}} \right] \overrightarrow{n_{ji}} \right\} \tag{13}$$

where $\overrightarrow{E_i^o}$ is the incident electric field on the ith particle, $\left\| \alpha \right\|_j$ the polarizability tensor of the particle j and $\overrightarrow{n_{ji}}$ is the unit vector from the jth to the ith particle. In (13), A_{ij} and B_{ij} are the interaction factors given by

$$A_{ij} = \left[k^2 - \frac{1}{r_{ij}^2} + \frac{ik}{r_{ij}} \right] \frac{\exp\left(ikr_{ij}\right)}{r_{ij}} \tag{14}$$

$$B_{ij} = \left[\frac{3}{r_{ij}^2} - k^2 - \frac{3ik}{r_{ij}} \right] \frac{\exp\left(ikr_{ij}\right)}{r_{ij}}. \tag{15}$$

In these equations, r_{ij} is the distance between the particle i and the particle j, and $k = 2\pi/\lambda$. Equation (13) can be written in a compact form as

$$\overrightarrow{E_i} = \overrightarrow{E_i^o} + \sum_{j \neq i}^{2N} \left\| C \right\|_{ij} \overrightarrow{E_j} \tag{16}$$

with $\left\| C \right\|_{ij}$ representing the interaction matrix between scatterers i and j. The problem now is reduced to solving the system of $6N$ coupled linear equations given by (16) with $6N$ unknowns, $\overrightarrow{E_i}$ $(i = 1, ...2N)$, which represent our final solution: the local field in every particle. One of the advantages of having the local fields is that it is possible to calculate the scattered field at every point in space. In particular, the total scattered far-field is given by

$$\overrightarrow{E_s} = \frac{k^2 \exp(ikR)}{R} \left(\left\| I \right\| - \overrightarrow{n_s} \overrightarrow{n_s} \right) \sum_{i=1}^{2N} e^{-ik\overrightarrow{n_s}\overrightarrow{r_i}} \left\| \alpha \right\|_i \overrightarrow{E_i} \tag{17}$$

where $\left\| I \right\|$ is the unit matrix, R is the distance from the sample to the detector $(kR \gg 1)$ and $\overrightarrow{n_s}$ is a unit vector indicating the scattering direction. Equation (16) may be rewritten in matrix form as

$$\overrightarrow{E} = \left(\left\| I \right\| - \left\| C \right\| \right)^{-1} \overrightarrow{E^o} \tag{18}$$

so the main calculation problem is the inversion of the complex matrix, $\|I\| - \|C\|$.

As an example of the application of the coupled-dipole method to analyze particle interaction, let us consider the scattering system of Fig. 1 with only two spherical particles separated by a distance d and located on a flat perfectly conducting substrate. This system is illuminated by a plane wave (S or P polarized) whose propagation direction is given by the angle of incidence, θ_i. The scattered field is measured in the plane of incidence at a scattering angle θ_s by means of an analyzer whose transmission direction is either perpendicular or parallel to this plane, i.e., we observe either the S or the P component of the scattered field respectively. The interaction effect between the two scatterers is a function of their separation d, the angle of incidence θ_i, and the polarization of the incident radiation. In order to quantify this effect, we define the depolarization coefficients given by

$$D_s(\theta_i, d) = \frac{\displaystyle\int_{-90^\circ}^{90^\circ} \langle I_{sp}(\theta_i, \theta_s, d)\rangle \, d\theta_s}{\displaystyle\int_{-90^\circ}^{90^\circ} \langle I_{ss}(\theta_i, \theta_s, d)\rangle \, d\theta_s} \tag{19}$$

$$D_p(\theta_i, d) = \frac{\displaystyle\int_{-90^\circ}^{90^\circ} \langle I_{ps}(\theta_i, \theta_s, d)\rangle \, d\theta_s}{\displaystyle\int_{-90^\circ}^{90^\circ} \langle I_{pp}(\theta_i, \theta_s, d)\rangle \, d\theta_s} \tag{20}$$

where $\langle\rangle$ stands for the average over all the possible relative orientations of the two particles. Because the scatterers have spherical symmetry and the scattered intensity is measured in the plane of incidence, the coefficients D_s and D_p are a measure of the amount of depolarized scattered light which appears in the plane of incidence due to particle interaction; i.e., they are a measure of the interaction.

Fig. 3 shows D_s and D_p as a function of the separation d between the two particles for two incident angles $\theta_i = 0^\circ$ and 60°. For comparison we have also included results when the substrate is absent in order to analyze the effect of its presence on the depolarization coefficients. The common feature of all these plots is that both D_s and D_p decrease as d increases. This is an obvious conclusion because the interaction is weaker when the particles are farther apart. However, it is important to point out that, with the substrate, the values of D_s and D_p are smaller than those with no substrate under the particles. Furthermore, the decrease in the depolarization coefficients is faster when the particles are very close ($d < 0.1\lambda$) than when they are far apart ($d > 0.4\lambda$). This means that the interaction effect only plays an important

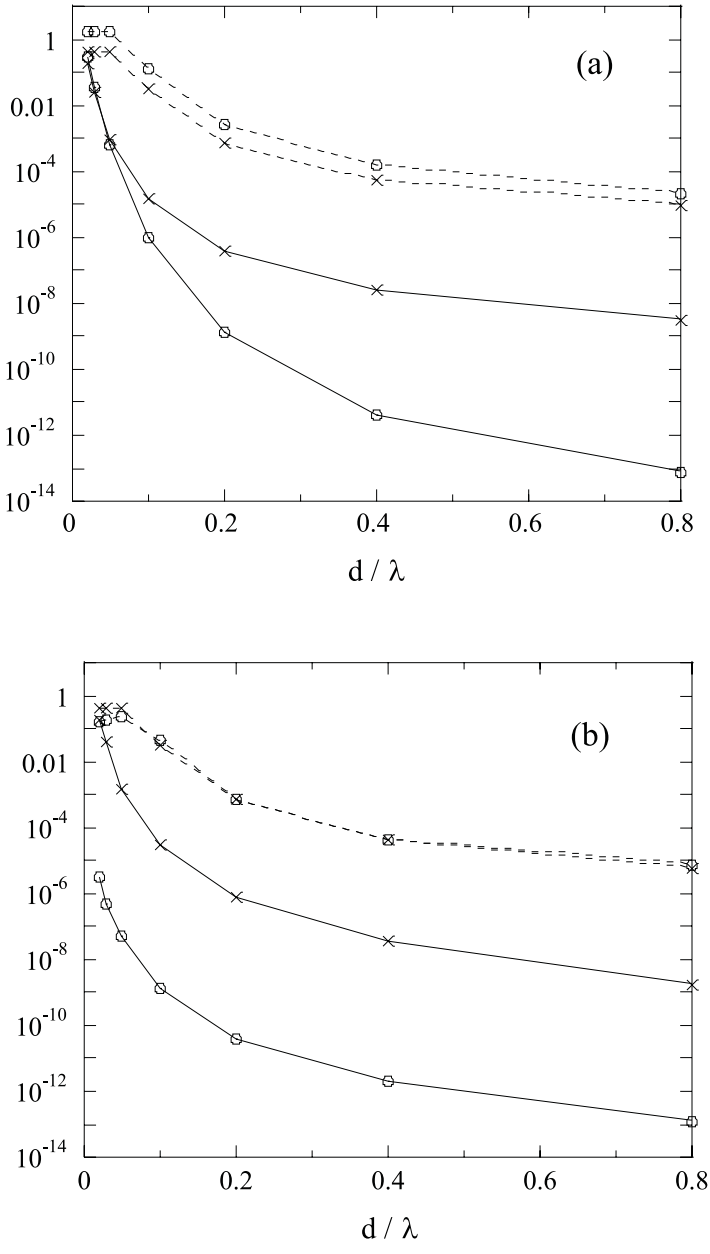

Fig. 3. The depolarization coefficients D_s (crosses) and D_p (circles)(see (19) and (20)) as a function of the relative separation, d/λ between the two scatterers, ($\epsilon = -2.01+0.001i$) for two angles of incidence, (a) $\theta_i = 0°$ and (b) $\theta_i = 60°$. Continuous line, with substrate; broken line, without substrate.

role when the particles are very close. This does not happen when there is no substrate. A detailed explanation of this can be found in [13].

Another interesting conclusion from Fig. 3 is that the presence of the substrate makes D_s and D_p behave differently. In particular the interaction is weaker for P incident polarization than for S incident polarization and decreases as the angle of incidence increases when the polarization of the incident light is parallel to the plane of incidence (P). When there is no substrate D_s and D_p show the same evolution regardless of both the separation between the particles and the angle of incidence.

Most of these results have been checked experimentally by the authors of this chapter and the reader may find further details in [14] and [15].

5 Intensity Fluctuations. Interacting Particles

In Sect. 3 the statistics of the light scattered by an ensemble of non-interacting particles has been briefly reviewed. In Sect. 4 the interaction between particles on a substrate has been analyzed. Now we have the tools to consider the central question of this chapter: how do the statistics change when the particles are interacting? In this section, we consider both isotropic and anisotropic particles and present the statistics for both co- and cross-polarized scattered light. Because of the theoretical complexity of the proposed problem, we resort to an empirical study through numerical simulations based on the IM and the CDM to extract the most interesting conclusions.

5.1 Isotropic Scatterers

a) Co-Polarized Scattered Light To study the effects of particle interaction, we have carried out some numerical simulations neglecting and including the effects of this interaction (see Fig. 4). The shape of the PDF of the co-polarized scattered intensity obtained in both cases is very similar, but some interesting differences appear. First, the PDF peaks are smoother. Second, a long tail appears for intensity values greater than $N^2 I_1$ (I_1 is the scattered intensity from one particle), which reaches very low probability values. This means that, in a series of intensity measurements, some peaks with very high intensity values occasionally appear. The strength of particle interaction has been varied by modifying the optical properties of the particles. For example, the closer they are to their resonance condition (ε_p=-2 , as can be deduced from (2) for ε_1=1), the more light they scatter and so the influence of one particle on its neighbors increases. We observed that intensity peaks greater than $N^2 I_1$, which show up as a consequence of particle interaction, increase in frequency and magnitude as the interaction between the particles increases. When this interaction is strong enough, the appearance of more frequent peaks with high values of the scattered intensity modifies the statistics significantly. In this case it is not possible to identify any characteristic shape

of the PDF, and its moments and their relative errors increase.These errors could be reduced by means of a good characterization of the PDF in the range of intensities $I > N^2 I_1$. However, the number of samples needed would be very high, and this is unpractical both from the numerical and experimental point of view.

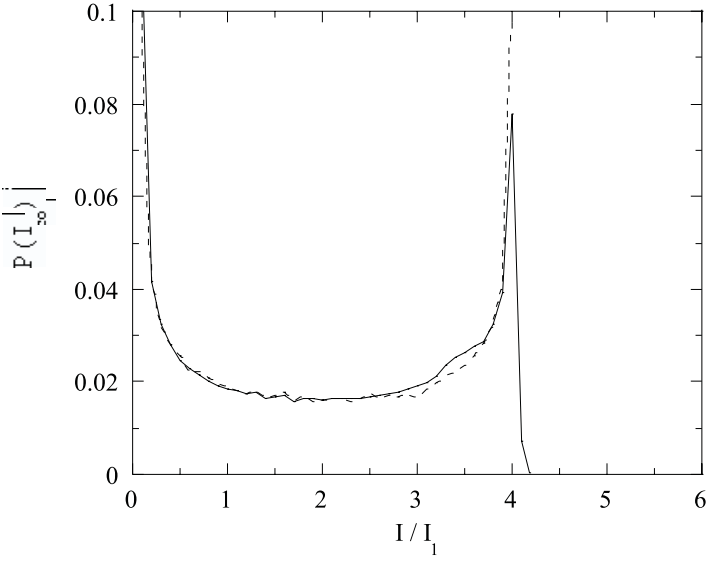

Fig. 4. PDF of the copolarized scattered intensity for two particles located on a flat substrate, neglecting (broken line) and including (continuous line) interaction effects

b) Cross-Polarized Scattered Light Scattered light from spherical particles in the plane of incidence whose polarization state is perpendicular to the incident one appears as a result of particle interaction. We show in Fig. 5 the cross-polarized intensity PDF when the mean number of illuminated particles is $\overline{N} = 5$ (N is Poisson-distributed) for spherical particles with radius $a = 0.05\lambda$ and dielectric constant ε_p=(-2.01,0). For all simulated cases, the statistics of the intensity fluctuations for the cross-polarization state have the same appearance. As can be seen, $P(I_{\text{cross}})$ has a maximum at $I_{\text{cross}} = 0$ and decreases dramatically as the intensity increases. We also observe that $P(I_{\text{cross}})$ remains finite even for values of I_{cross} much greater than the mean scattered intensity. This means that, when looking at the fluctuations, some peaks of very high intensity occasionally appear which are caused by the presence of two or more particles very close to each other. The corresponding moments also have very high values, and their relative errors always exceed 90%. Therefore, the information we may obtain by analyzing them is not

trustworthy. As an alternative, we propose measuring only one specific value of $P(I_{\text{cross}})$. In particular, this measurement was chosen for $P(I_{\text{cross}} = 0)$ because at that point the PDF (Fig. 5) shows the smallest relative error and also because this parameter can be used to quantify particle interaction: $P(I_{\text{cross}} = 0) = 1$ when there is no particle interaction, and decreases as interaction increases.

We have developed a very simple model to study the dependence of $P(I_{\text{cross}} = 0)$ with the number of illuminated particles. We assume that the particle surface density is constant on the surface (N is a Poisson-distributed random variable). We also assume that there is a threshold intensity I_0 below which we cannot detect any scattered intensity, so that for $I_{\text{cross}} < I_0$, we consider $I_{\text{cross}} = 0$ (this is indeed the case when carrying out any real experiment in the laboratory). If a particle scatters a cross-polarized intensity I_0 when it is separated by a distance L from its nearest neighbor, the probability of detecting zero cross-polarized intensity from that particle is the probability of it being separated from its nearest neighbor by a distance greater than L,

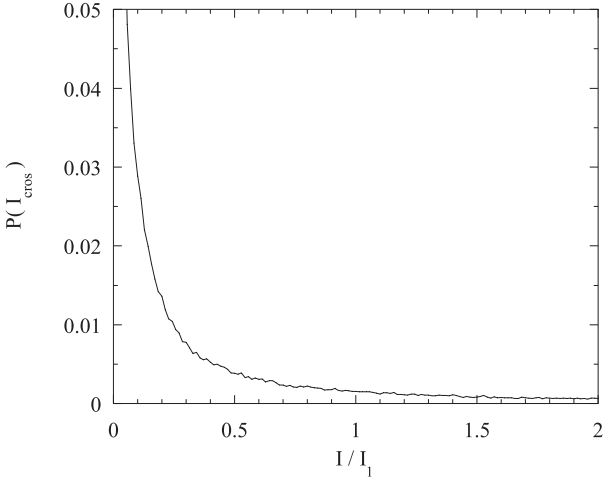

Fig. 5. PDF of the cross-polarized scattered intensity for spherical particles with $a = 0.05\lambda$ and $\epsilon_p = (-2.01, 0)$. $\overline{N} = 5$.

$$P_i(I_{\text{cross}} = 0) = P_i(d > L) = \int_L^{\infty} \frac{1}{\sigma} \exp(-\sigma l) dl = \exp(-\sigma L) \tag{21}$$

where σ can be identified as a particle linear density on the surface ($\sigma = \sqrt{\overline{N}/\pi R^2}$, R being the radius of the illuminated area). The probability of

getting zero cross-polarized scattered intensity when the number of illuminated particles is $\overline{N}$ is then

$$P(I_{\text{cross}} = 0) = [P_i(I_{\text{cross}} = 0)]^{\overline{N}} = \exp\left(-L\sqrt{\frac{\overline{N}^3}{\pi R^2}}\right) \tag{22}$$

The parameter L, which is the maximum interparticle distance at which interaction effects can be detected, can be determined by performing a curve-fit carried out for surfaces contaminated with the same kind of particles. This parameter should depend not only on the particle characteristics (size, shape and optical properties) but also on both the illumination and detection parameters (incidence and scattering angles and polarization of the incident and scattered radiation). This model explains the behavior observed in our numerical results. As an example, we show in Fig. 6 the dependence of $P(I_{\text{cross}} = 0)$ with $\overline{N}$, when the particles have a dielectric constant ε_p=(-2.01,0) and radii $a = 0.05\lambda$ (crosses), 0.07λ (squares) and 0.1λ (circles). The marked points correspond to the simulated data and the curves show their fit to (22). The calculated values for L are 0.33λ, 0.79λ and 0.83λ, respectively. This result is consistent with the model because it means that as particle size increases, the maximum interparticle distance at which multiscattering effects can be detected also increases.

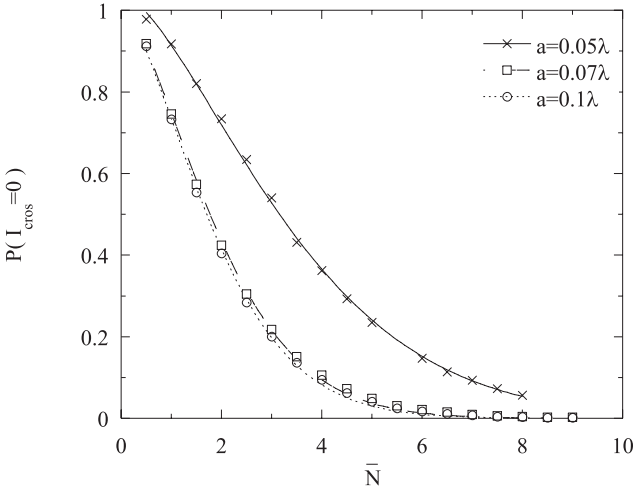

Fig. 6. $P(I_{\text{cross}} = 0)$ as a function of $\overline{N}$ for substrates contaminated by particles with different radii a and $\epsilon_p = (-2.01, 0)$.

Interest in this model is more theoretical than practical. This is because in the laboratory it is very difficult to get a set of flat substrates contaminated with the same kind of particles, with different, homogeneous and known particle surface densities. Usually there is only one sample from which we can extract as much information as possible. It is then more practical to express (22) in the form

$$P(I_{\text{cross}} = 0) = \exp\left[-\left(L\pi\sigma^3\right) R^2\right] = \exp(-\gamma R^2) \tag{23}$$

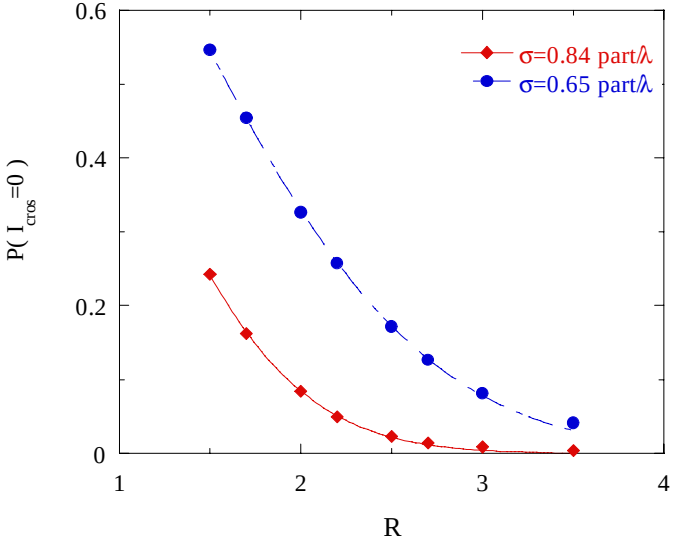

Fig. 7. $P(I_{\text{cross}} = 0)$ as a function of the radius of the illuminated area R, for two surfaces contaminated by spherical scatterers ($a = 0.05\lambda$ and $\epsilon_p = (-2.01, 0)$) with different particle surface density, σ.

Therefore, in these cases we should measure the dependence of $P(I_{\text{cross}} = 0)$ with the illuminated area. Figure 7 shows $P(I_{\text{cross}} = 0)$ as a function of the radius of the illuminated area R for two different surfaces with the same kind of particles (spherical, with $a = 0.05\lambda$ and ε_p=(-2.01,0)) whose linear particle densities are $\sigma = 0.84$ and $\sigma = 0.65$ particles/λ. The marked points are the simulated results, and the curves show the fit to (23). Following this method, we can calculate L for a given value of σ (in our case, the relative error in this calculation is 1% with respect to the previously obtained value) and vice versa. This fit is also useful to determine the linear particle density ratio between two different surfaces contaminated by the same kind of particles.

According to (23), this ratio is

$$\frac{\sigma_1}{\sigma_2} = \left(\frac{\gamma_1}{\gamma_2}\right)^{1/3} \tag{24}$$

From the numerical results shown in Fig. 7, we obtain $\sigma_1/\sigma_2 = 1.312$. This allows us to calculate σ_2 if σ_1 is known, with a relative error of 1.6%. Once we have a well characterized sample, it can be used to determine the linear particle density of other samples contaminated by the same kind of particles.

5.2 Non-isotropic Scatterers

In this section we examine the fluctuations of the scattered light from flat substrates contaminated by spheroidal particles. Their particle shape is characterized by the ratio between their two main axes, $r = d_1/d_2$. Depending on this value, three different kinds of particles can be distinguished: spherical particles ($r = 1$), oblate particles ($r < 1$) and prolate particles ($r > 1$). In the calculations presented in this section, the particles have a dielectric constant ε_p=(-2.01,0) and $d_2 = 0.05\lambda$ (d_1 varies with r). We also assume that as the particles settle down on the substrate, prolate particles have their largest axis parallel to the substrate, while the shortest axis of the oblate particles aligns perpendicularly to the substrate.

a) Co-Polarized Scattered Light Figure 8 shows the PDF of the co-polarized scattered light for oblate particles (on the left) and prolate particles (on the right), when the number of illuminated particles is assumed to be constant: $N = 2$ (two upper graphs) and $N = 3$ (two lower graphs). The scattered intensity has been normalized to its mean value. These results are quite different from those presented by Bates *et al.* (compare them with Fig. 1 of [16]), who studied the fluctuations of the scattered intensity from an ensemble of spheroidal particles, disseminated in a volume, and whose interaction was neglected. The difference is due to the effect of the presence of the substrate on the particle orientation; this gives them a preferential alignment. If we eliminate the substrate, allowing the particles to have an arbitrary orientation; we recover the results presented in [16].

We observe in Fig. 8 that oblate particles present the same PDF independently of the value of r, and this PDF coincides with the PDF obtained for spherical particles ($r = 1$). This is a direct consequence of the alignment imposed by the presence of the substrate. Because of this alignment, every particle scatters the same amount of light, so that their superposition only depends on the relative positions of the particles (as was the case with spherical particles). The only difference in the light scattered from oblate particles with different r is the value of the mean intensity, which cannot be seen in

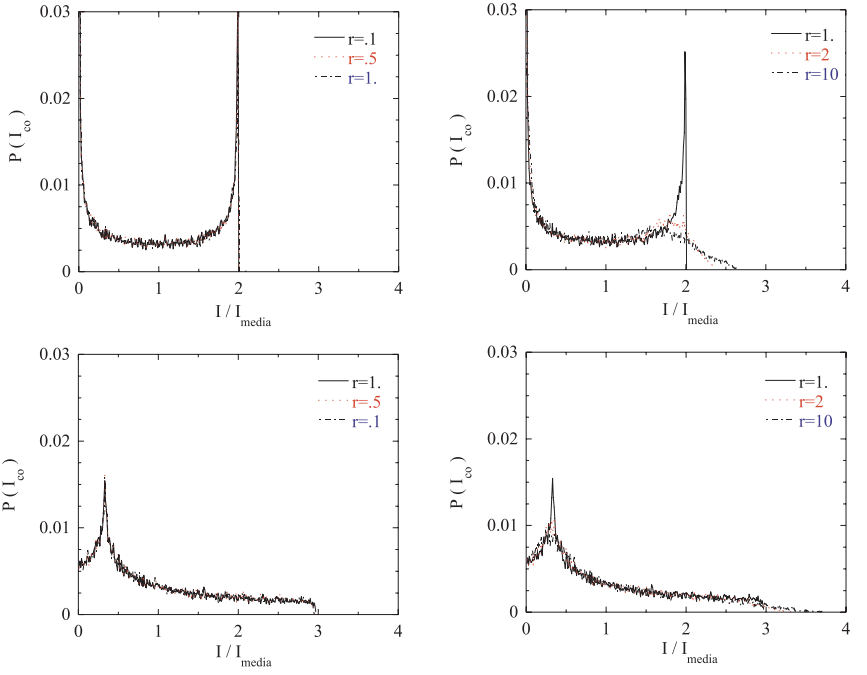

Fig. 8. PDF of the copolarized scattered intensity for oblate (two left plots) and prolate (two right plots) particles. $N = 2$ for the two upper plots and $N = 3$ for the two lower ones.

Fig. 8. When r decreases, d_1 (and consequently α_1) decreases; therefore, the amount of scattered light from each particle also decreases which makes the total scattered intensity smaller. The result is quite different for prolate particles on the substrate. In this case the resulting PDF is different from that obtained for spherical particles, and its shape depends on the parameter r. This is because in this case the amplitude of the total scattered field depends not only on the particle relative positions, but also on the orientation of each particle on the substrate. As a consequence, the shape of the PDF is smoother.

b) Cross-polarized scattered light Oblate particles have a polarizability tensor that is diagonal in the laboratory system because of their alignment on the substrate. This means that if there is only one particle on the substrate, it cannot scatter light with polarization perpendicular to that of the incident beam, so this component can only appear as a consequence of particle interaction. The behavior of the fluctuations of the cross-polarized scattered intensity must then be analogous to that observed for spherical particles. We have checked that $P(I_{\text{cross}})$ and its normalized moments really do show the

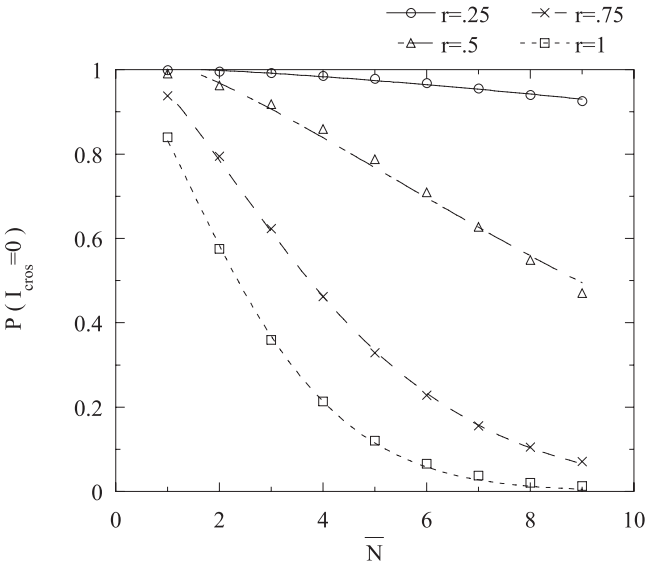

Fig. 9. $P(I_{\text{cross}} = 0)$ for oblate particles of different shapes (different values of r) as a function of $\overline{N}$. The marks show the simulated data and the lines, their fits to the model (see (22)).

same behavior described for spherical particles and so all the previous conclusions can be extended to substrates contaminated by oblate particles. We can also extend the model to study the dependence of $P(I_{\text{cross}} = 0)$ on the number of particles in the illuminated area. Figure 9 shows this evolution for oblate particles with different shape ratios r. The fitted values for the parameter L show that they increase as r increases. This is because when r increases, the height of the dipole (located at the center of the particle) and the polarizability component perpendicular to the substrate also increase and so particle interaction becomes stronger.

The polarizability tensor of prolate particles has non-null off-diagonal elements in the laboratory system; therefore, these particles are able to scatter cross-polarized light in the plane of incidence by themselves, even when there is no particle interaction. Figure 10 shows the PDF of the cross-polarized scattered intensity for prolate particles of different shapes when the number of illuminated particles is assumed to be constant. As predicted, its behavior is quite different from that observed for both oblate and spherical particles. The PDF shape does not vary with the ratio r, and so it is not possible to distinguish between surfaces contaminated by prolate particles with different shapes. In contrast to what happens with oblate particles, the normalized moments of this distribution can be determined with a very small relative error. To distinguish between surfaces with prolate and oblate particles, measuring

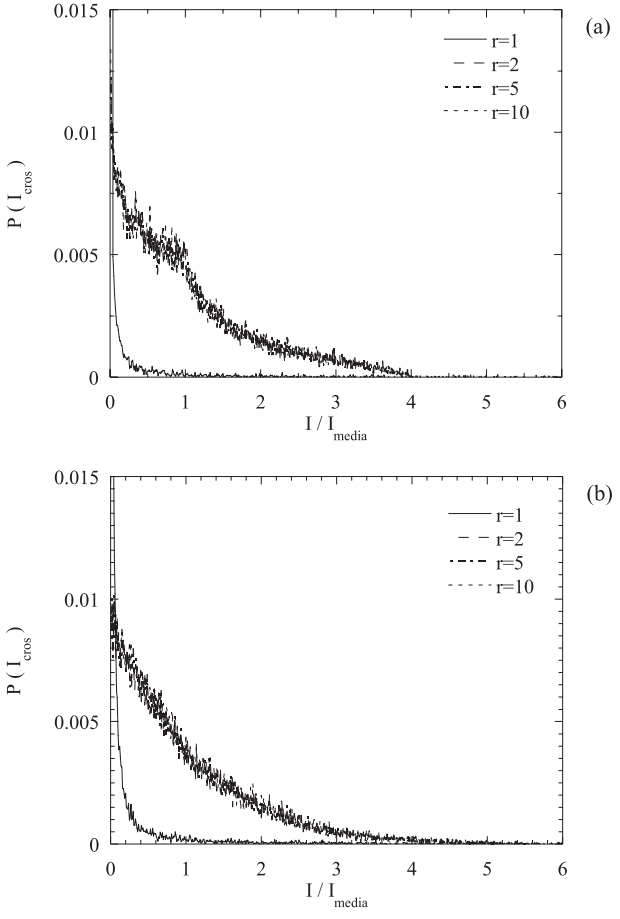

Fig. 10. PDF of the cross-polarized scattered intensity from prolate particles for different values of r. Part (a) corresponds to $N = 2$ and (b) to $N = 3$. N is assumed constant.

these moments is probably more effective than analyzing the PDF shape of the co-polarized intensity. This is because the shape of these PDFs is very smooth, so the recognition of characteristic features is a difficult task.

Figure 11 shows the dependence of the second (upper graph) and third (lower graph) normalized moments as a function of the mean number of illuminated particles $\overline{N}$. The dependence does not compare well with that predicted in (12) because this equation was deduced for isotropic particles (spherical or oblate particles when they are aligned on the substrate). When the particles are prolate, the amplitude of the scattered field from each particle depends on the orientation of the particle with respect to the reference

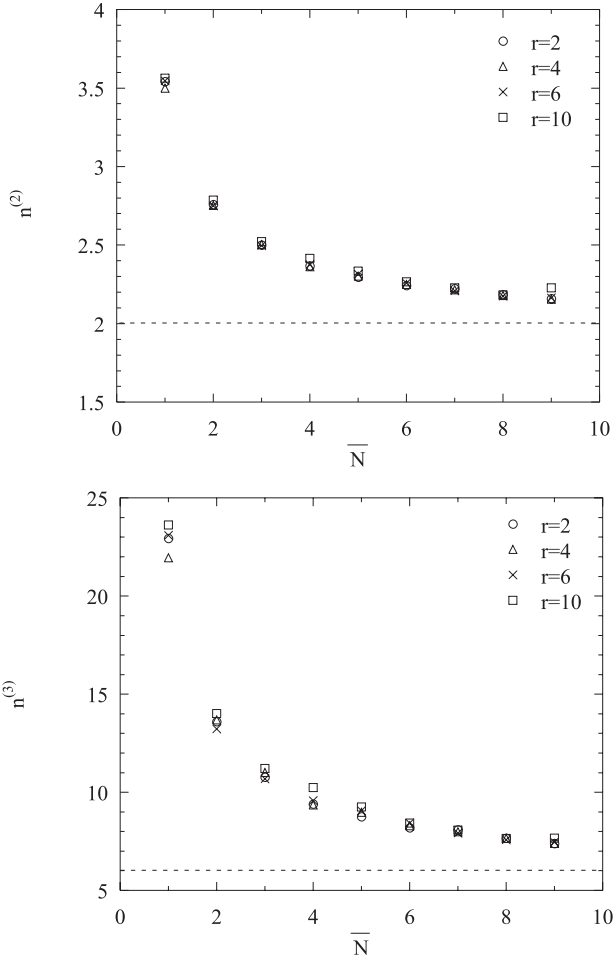

Fig. 11. $n^{(2)}$ and $n^{(3)}$ of the fluctuations of the cross_polarized scattered intensity from prolate particles as a function of $\overline{N}$ for different values of r. The horizontal lines show the values predicted for Gaussian statistics.

system. This modifies the statistics and consequently the corresponding moments [17].

6 Acknowledgments

The authors wish to thank the Dirección General de Enseñanza Superior for its financial support (project PB97-0345). Eva M. Ortiz wishes to thank to the Vice-Rector of Research of the University of Cantabria for her grant.

References

1. Dainty J.C. (1984) Laser Speckle and Related Phenomena, 2nd edn. Springer, Berlin
2. Jakeman E., Tough R.J.A. (1988) Non-Gaussian Models for the Statistics of Scattered Waves. Adv. Phys. 37:471-529
3. Lilienfeld P. (1986) Optical Detection of Particle Contamination on Surfaces: A Review. Aerosol Science and Technology 5:145-165
4. Pidduck A.J., Robbins D.J., Young I.M., Cullis A.G., Martin A.S.R. (1989) Materials Science and Engineering B4:417-422
5. Freeman R.G., Grabar K.C., Allison K.J., Bright R.M., Davis J.A., Guthrie A.P., Hommer M.B., Jackson M.A., Smith P.C., Walter D.G., Natan M.J. (1995) Self-Assembled Metal Colloid Monolayers: An Approach to SERS Substrates. Science 267:1629-1632
6. Jakeman E. (1994) Scattering by Particles on an Interface. J. Phys. D: Appl. Phys. 27:198-210
7. Van de Hulst H.C. (1981) Light Scattering by Small Particles. Dover, New-York
8. Bohren C.F., Huffman D.R. (1983) Absorption and Scattering of Light by Small Particles. Wiley, New-York
9. Soto-Crespo J.M., Nieto-Vesperinas M. (1989) Electromagnetic Scattering from very Rough Random Surfaces and Deep Reflection Gratings. J Opt Soc Am A 6:367-384
10. Rayleigh L. (1912) On the Light Dispersed from Fine Lines Ruled upon Reflecting Surfaces or Transmitted by very Narrow Slits. In: Scientific Papers. Cambridge University, Cambridge
11. Pusey P.N. (1977) Statistical Properties of Scattered Radiation. In: Cummins H.Z., Pike E.R. (Eds.) Photon Correlation Spectroscopy and Velocimetry. NATO ASI Series: Series B, Physics. Plenum Press, New-York. 23:45-141
12. Singham S.B., Bohren C.F. (1988) Light Scattering by an Arbitrary Particle: The Scattering-Order Formulation of the Coupled-Dipole Method. J Opt Soc Am A 5:1867-1872
13. Moreno F., Saiz J.M., Valle P.J., González F. (1995) On the Multiple Scattering Effects for Small Metallic Particles on Flat Conducting Substrates. Waves in Random Media 5:73-88
14. González F., Saiz J.M., Valle P.J., Moreno F. (1995) Scattering from Particulate Metallic Surfaces: Effect of Surface Particle Density. Opt Eng 34:1200-1207
15. González F., Saiz J.M., Valle P.J., Moreno F. (1997) Multiple Scattering in Particulate Surfaces: Cross-Polarization Ratios and Shadowing Effects. Opt Comm 137:359-366
16. Bates A. P., Hopcraft K. I., Jakeman E. (1997) Particle Shape Determination from Polarization Fluctuations of Scattered Radiation. J Opt Soc Am A 14:3372-3378
17. Jakeman E. (1995) Polarisation Fluctuations in Radiation Scattered by Small Particles. Waves in Random Media 5: 427-442